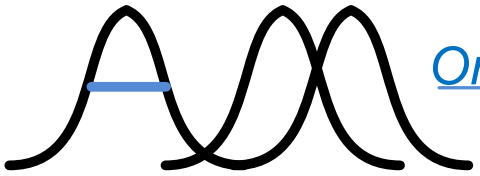

Photogrammetry for Non-Invasive Terrestrial Position/Velocity Measurement of High-Flying Aircraft

Part III: Direct-Drive Motor Chassis Design & Assembly

James A Crawford

Synopsis

Part I provided a simple introduction to the big-picture objectives for this multi-phase project.

Part II first looked at telescope mounts, ultimately focusing on the azimuth-elevation type mount for the project. The basic mathematics for dealing with 3-phase DC motors (e.g., Clarke and Park transformations) were introduced, along with the first ingredients for modeling and controlling the DC motors in a precision manner. The *Launchpad* hardware platform from Texas Instruments was selected to host the motor control algorithms.

In this project installment (Part III), most of the attention is focused on the design and assembly of the telescope mount. The detailed design of the hardware changed appreciably from the first concept as better approaches were recognized during the detailed design.

With the assembly of most of the telescope mount now completed, we can at last start taking a peek at the motor's characteristics and start ramping on the electronic control aspects of this project.

1 Getting Started

In Part II of this project, the main hardware ingredients of the Azimuth DC motor were introduced as shown in Figure 1 and the beginnings of a supporting CAD package were presented as shown in Figure 2. A rather ad-hoc control system including a mathematical model for the DC motor was suggested as shown in Figure 3. As already mentioned in the synopsis, this project installment is primarily focused on the mechanical design, fabrication and assembly of the telescope mount.

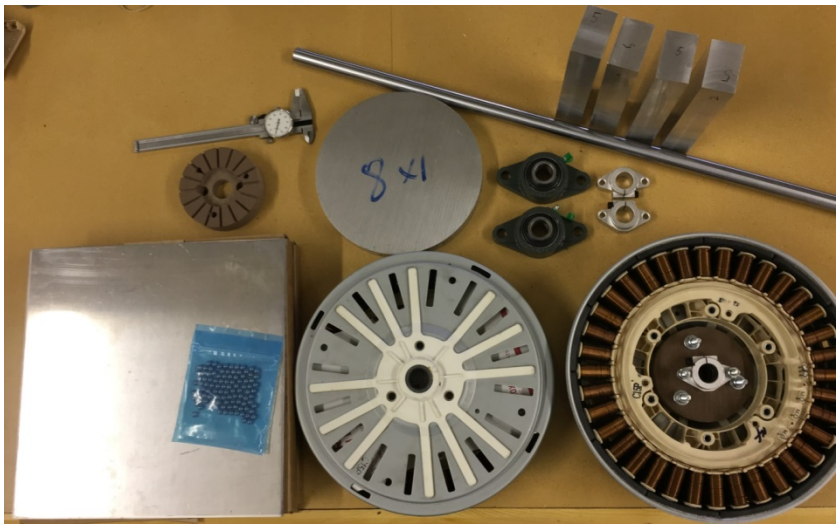

Figure 1 Most of the materials needed for the azimuth drive motor portion. The four rectangular bars in the upper right-hand corner will serve as spacers for the top and bottom plates of the azimuth motor housing. For practice, they were milled to an accuracy of about 0.0005” on all six faces. The 8” aluminum disk was milled into the azimuth turn-table.

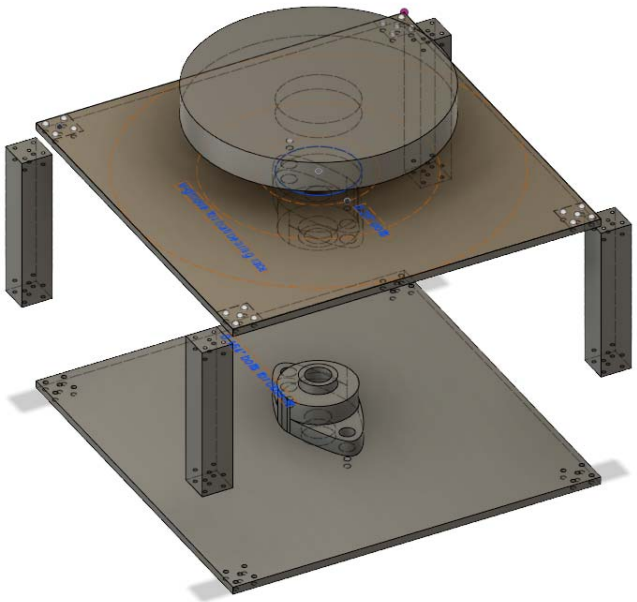

Figure 2 Fusion 360 CAD drawing of the azimuth motor section in progress

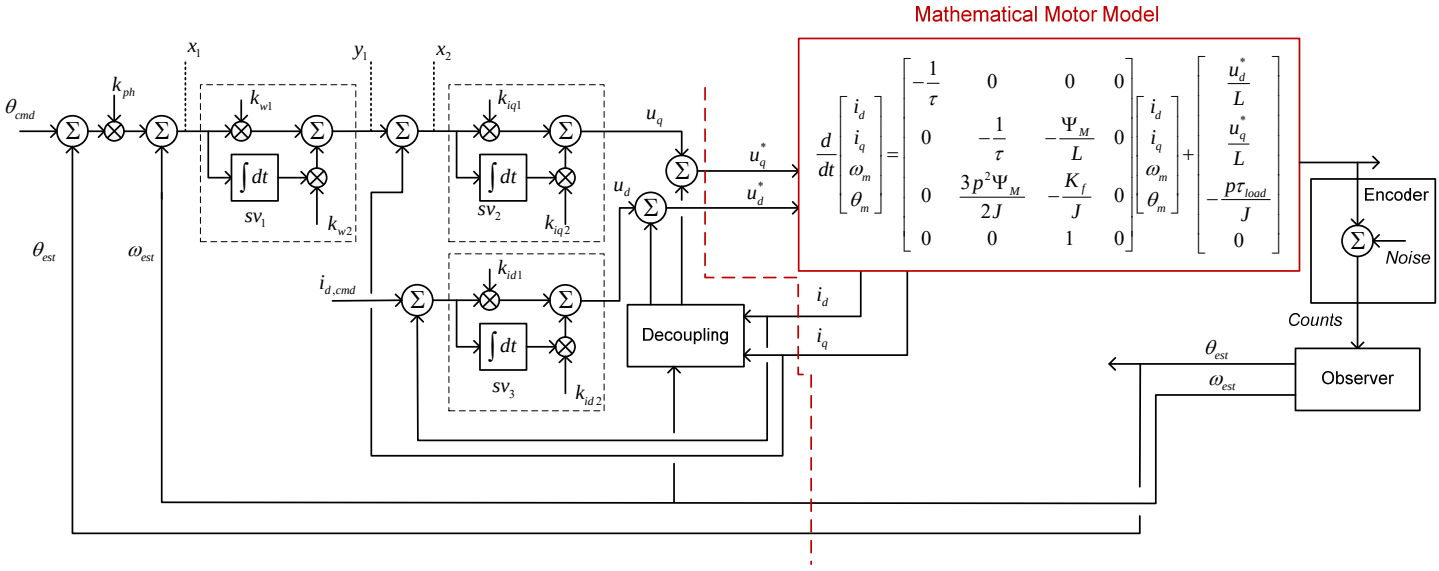

Figure 3 First-cut control system model for the Azimuth DC motor controller[1]

2 Azimuth Mount Mechanical Design

The mechanical design and fabrication of my mount thus far is shown in Figure 4. There are more components involved than meet the eye, and when one considers that even a simple cube has up to 6 faces that may need to be machined, the number of milling setups grows quickly. Over 100 different setups have been used thus far.

Figure 4 Az-El telescope mount design and fabrication progress thus far

[1] U25073 Photogrammetry Part II Figures.vsd.

As I launched into the detailed mechanical design from Figure 1 and Figure 2, there were several aspects that I found unappealing:

- the pillow bearings were very large, particularly in height, which was going to grow the height of the azimuth mount portion more than desired
- it became clear that some bearing features could be more closely integrated into the mechanical housing itself thereby reducing the overall height further

Given these observations, I abandoned the pillow block bearings in favor of much smaller bearings from VXB. All of the mechanical design was done using Fusion 360 as an example in Figure 5 and Figure 6 demonstrate. The final milled pieces are shown with a 20 mm precision VXB bearing installed in Figure 7 and Figure 8.

Rather than go through all of the details associated with the design, a sequence of assembly photos is provided here in Figure 9 through Figure 21.

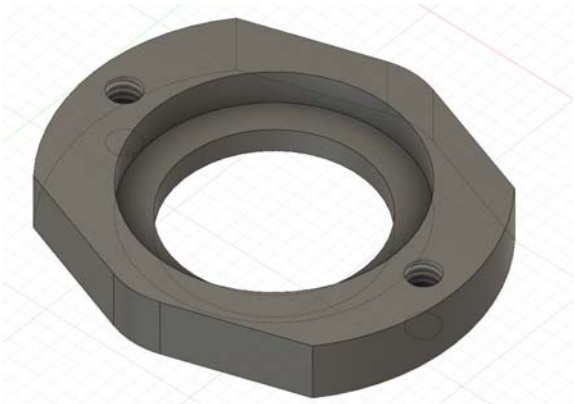

Figure 5 Fusion 360 design of top portion of VXB bearing mount

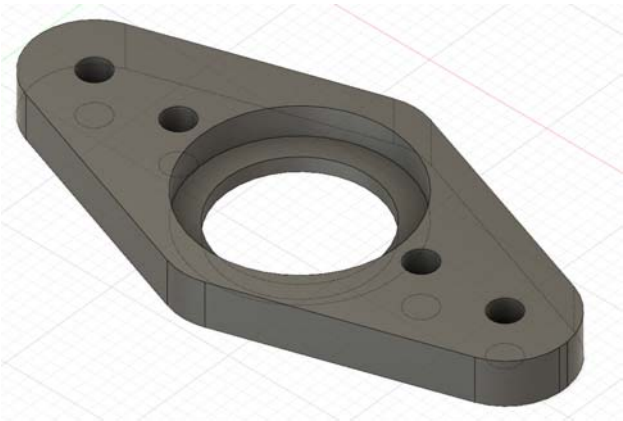

Figure 6 Lower portion of VXB bearing mount

Figure 7 Bottom portion of VXB bearing with VXB bearing situated

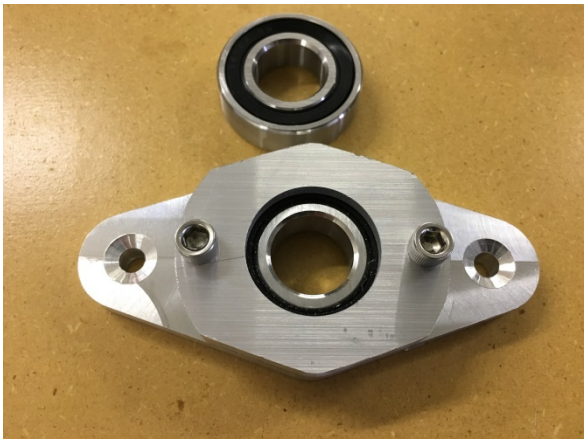

Figure 8 VXB bearing sandwiched between the bearing holder pieces, with an extra bearing shown top

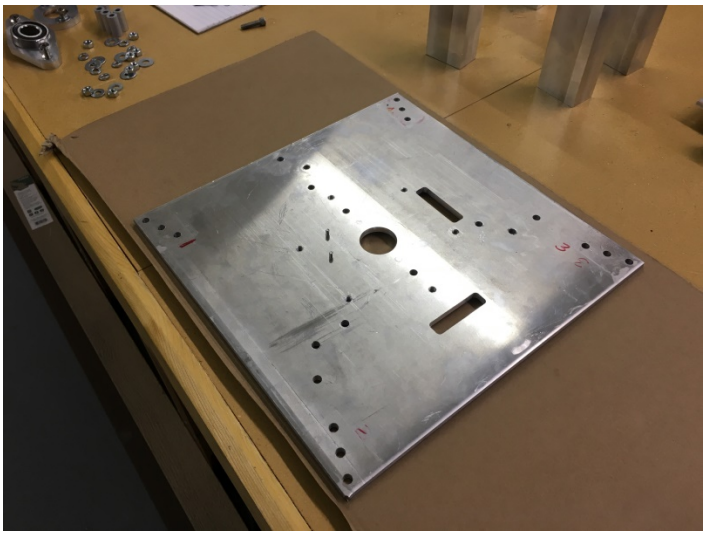

Figure 9 Azimuth mount, bottom plate

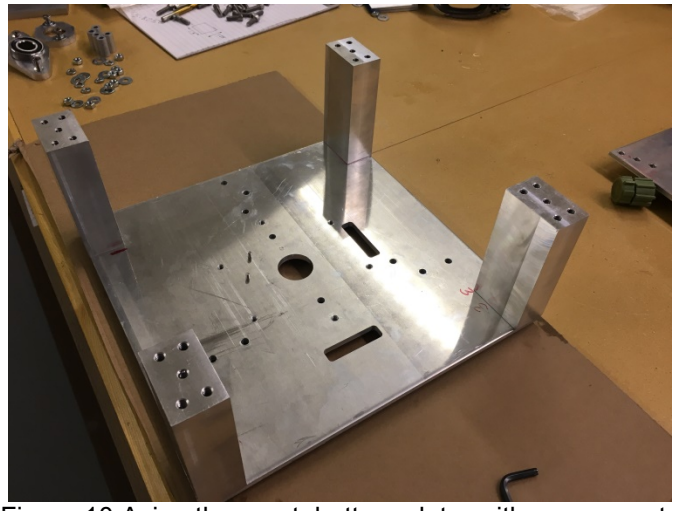

Figure 10 Azimuth mount, bottom plate, with corner posts installed

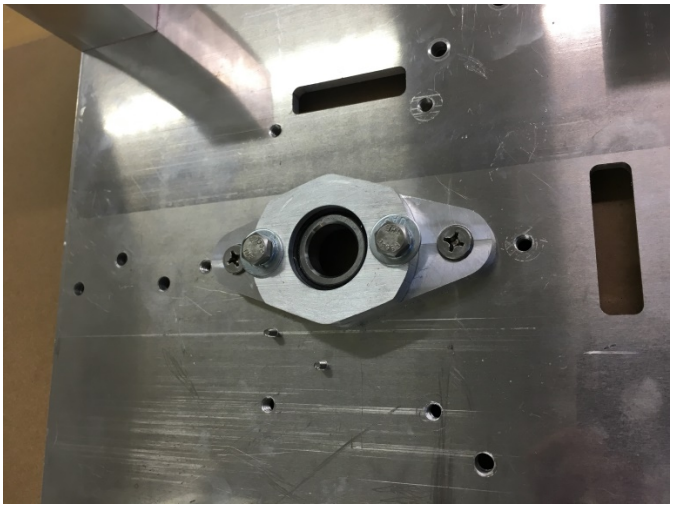

Figure 11 Azimuth mount with corner posts and center bearing installed

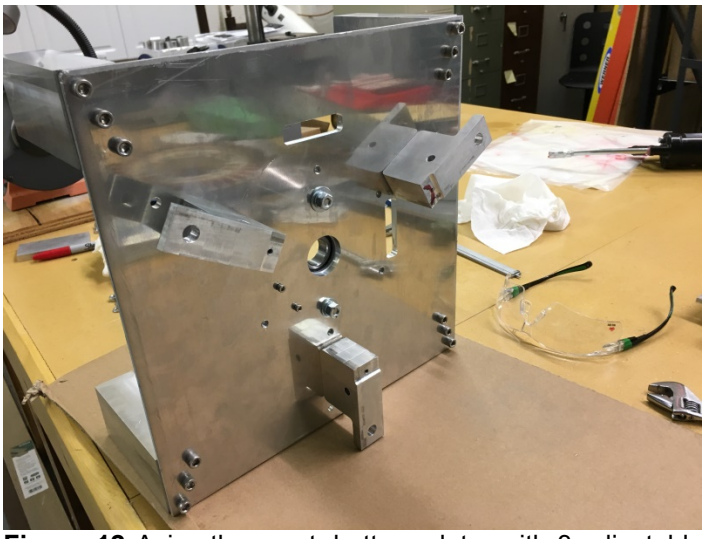

Figure 12 Azimuth mount, bottom plate, with 3 adjustable feet installed. The large hole in each foot will be used if a 3-point pier is used for the overall mount whereas the smaller perpendicular hole in each foot will accommodate a tripod if the choice is ultimately made.

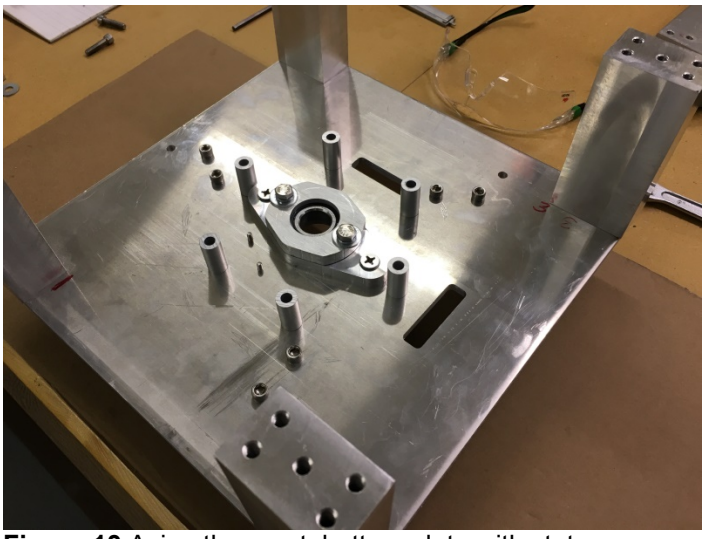

Figure 13 Azimuth mount, bottom plate with stator spacers

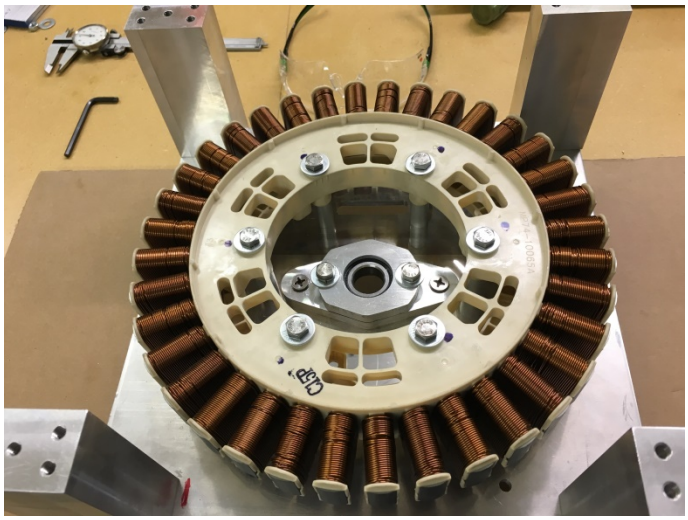

Figure 14 Azimuth mount, bottom plate, now with stator installed

Figure 15 Machined shaft

Figure 16 Machined axle collar for shaft absent threaded set-screw holes for holding the collar in place

Figure 17 Axle, bearing assembly and collar in place on the under-side of the top plate

Figure 18 Second perspective of Figure 17

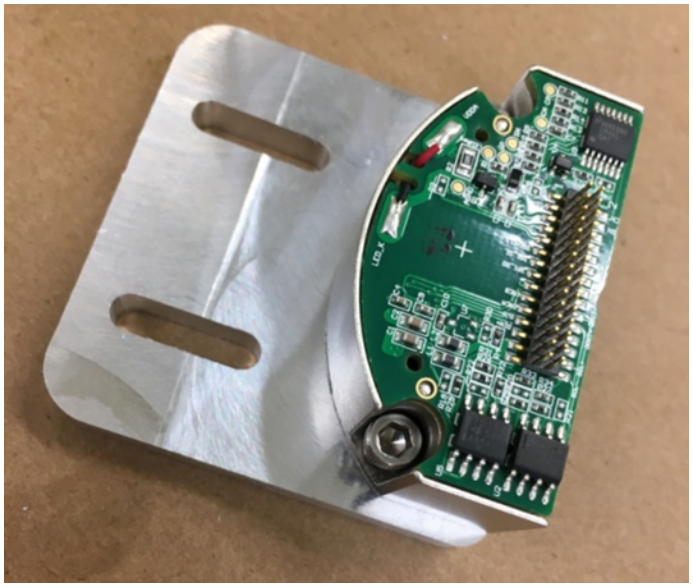

Figure 19 Optical encoder electronics hosted by the machined alignment fixture

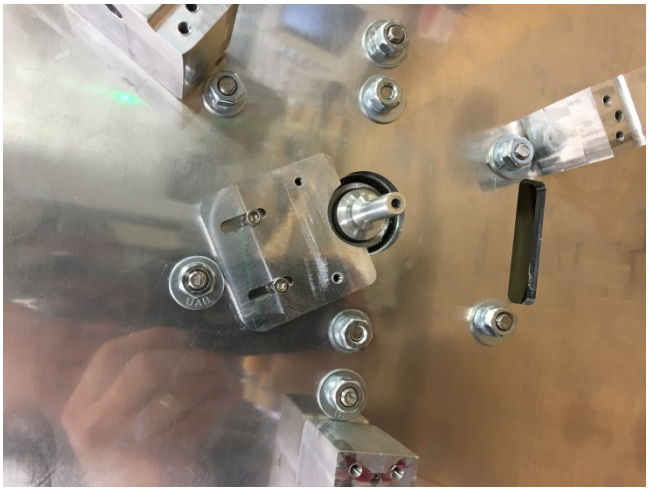

Figure 20 Bottom side showing the 3 offset feet, tapered azimuth axle and optical encoder mount

Figure 21 Azimuth mount portion, largely completed and testing back-EMF behavior. Turn-table will host the elevation portion of the mount.

Figure 22 Elevation yoke taking shape. Two more VXB precision bearings used for the elevation axis.

Figure 23 Mount with telescope installed temporarily. Optical encoder to be installed on the near-side of the yoke.

Figure 24 Newly milled telescope ring mounts

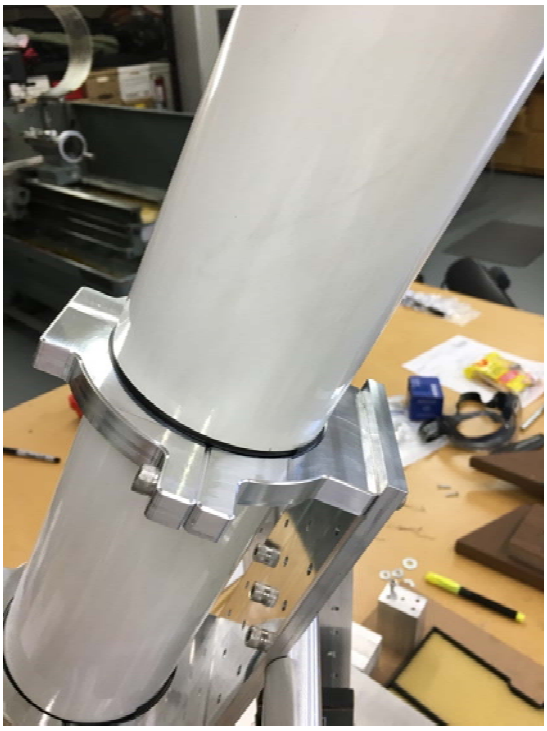

Figure 25 Close-up of one telescope ring mount attached to saddle with telescope in place

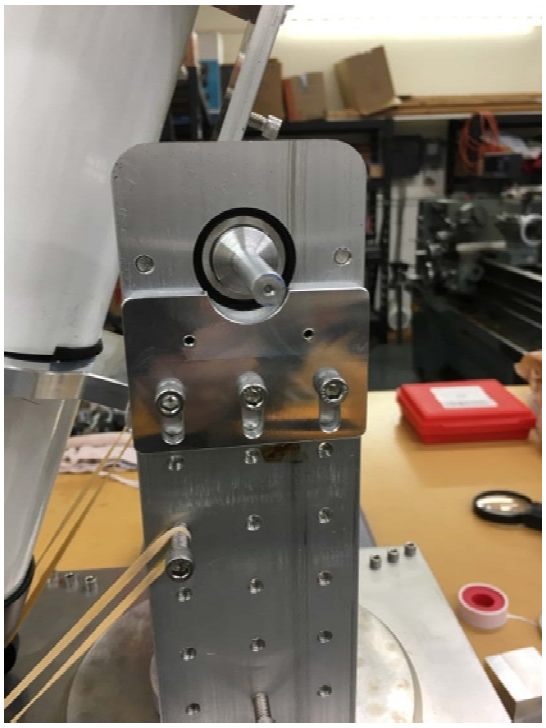

Figure 26 Elevation axle optical encoder mount in place

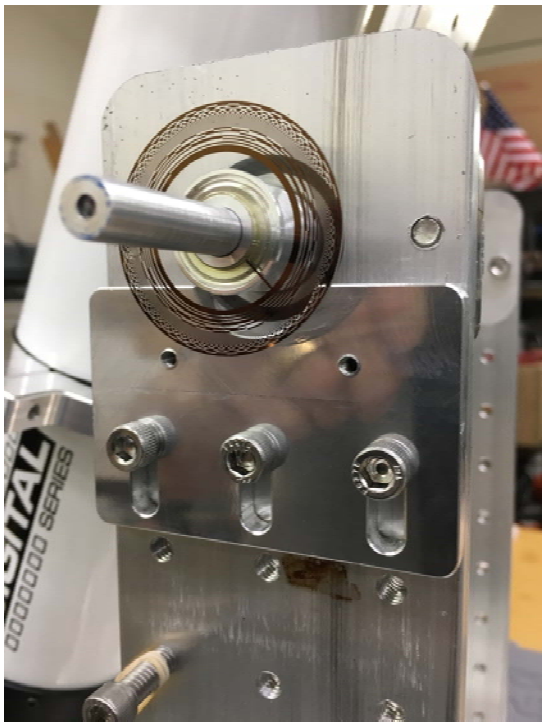

Figure 27 Optical encoder wheel on the elevation axle

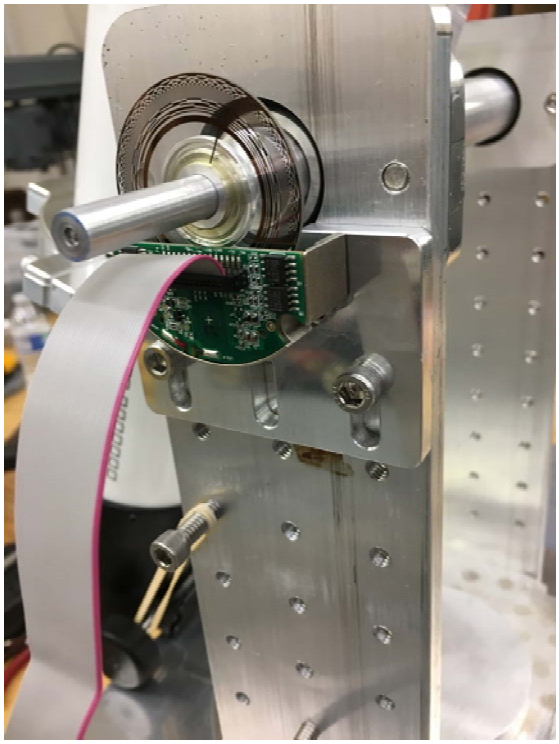

Figure 28 Optical encoder wheel, optical encoder readout installed on the adjustable encoder mount. A protective cover will complete the assembly.

3 Azimuth Motor Characterization

I have virtually zero information about the Samsung motor being used in this project for the azimuth drive aside from the following information:

- 3-phase design
- 36 poles
- physical diameter about 12 inches
- Samsung DC31-00111A stator, DC31-00112A rotor
- details provided in §3.1 of Part II [2]

Section 3.1 of Part II [2] also contained a general discussion about cogging torque and characterization of electrical motors in general.

Having the assembled azimuth mount portion in-hand now (Figure 21), casual inspection reveals the fairly severe nonlinear torque aspects of the motor at start-up and very low rotational speeds (e.g., < 5 RPM). A two-channel oscilloscope was set up as shown in Figure 21 to observe the open-circuit voltage across the two pairs of 3-phase inputs (one terminal served as the common reference) as the motor was turned by hand. At low rotational speed (about 2 RPM), the open-circuit voltage signatures are very distorted and anything but sinusoidal as shown in Figure 29. Increasing the rotational speed to about 8 RPM brings about the onset of much more sinusoidal behavior as shown in Figure 30. It is also worth noting the fairly high peak-to-peak voltage swing of 20V in Figure 30 due in part to the 36-pole nature of the permanent magnet motor.

Another fun but expected observation with the setup in Figure 21 was the rotational counter-force observed when one pair of stator terminals was shorted. This increased the resisting cogging torque by perhaps as much as 5x while retaining the jerky rotational characteristics of the open-circuit configuration. When all three stator terminals were shorted together, the rotational counter-force was on the order of 10x stronger than in the open-circuit condition and no evidence of periodic cogging behavior was perceivable.

As anticipated, the nonlinear nature of the cogging torque will likely press my algorithm design skills as I get into the control loop aspects of the project. B

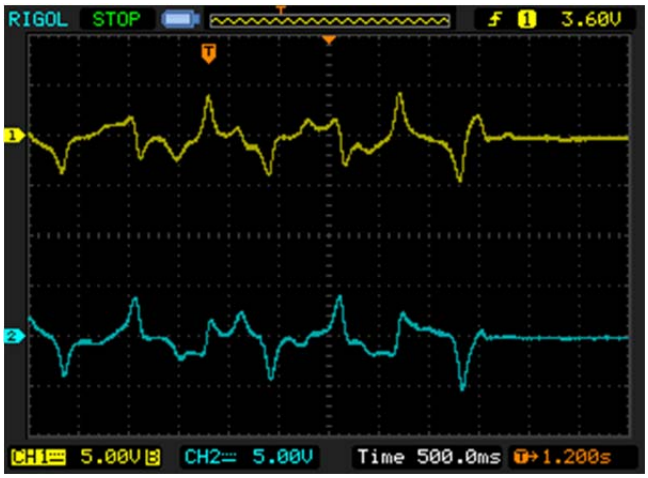

Figure 29 Open-circuit 2-phase difference voltages at about 2 RPM, motor turned by hand

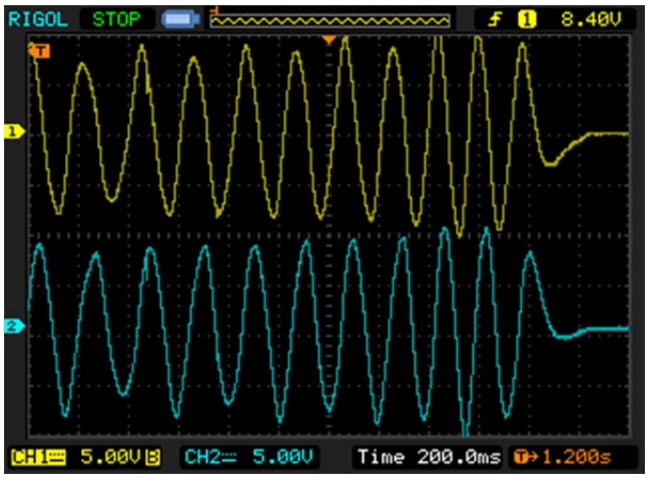

Figure 30 Open-circuit 2-phase difference voltages at about 8 RPM, motor turned by hand. Each cycle represents turning the motor one pole-spacing or about 10^{o}.

4 Wrap-Up

I originally intended to have more results in this project installment pertaining to the control theory aspects of the design. But as is usually the case, progress was slower than desired. Perhaps my major accomplishments over these past months has been getting very comfortable with my Haas TM-1P milling machine and getting proficient with the Fusion 360 CAD software I have used throughout the mechanical design to date.

5 References

1. J.A. Crawford, “Photogrammetry for Non-Invasive Terrestrial Position/Velocity Measurement of High-Flying Aircraft, Part II: Direct-Drive Motors,” U24933, 23 April 2019.
2. _____, “Photogrammetry for Non-Invasive Terrestrial Position/Velocity Measurement of High-Flying Aircraft, Part I: Direct-Drive Motors,” U24933, 16 October 2017.
3. Texas Instruments, “LAUNCHXL-F28379D Overview, User’s Guide,” SPRUI77A, August 2017, U25038.
4. Matthew Piccoli and Mark Yim, “Cogging Torque Ripple Minimization via Position-Based Characterization,” U25085.
5. P.W. Poels, “Cogging Torque Measurement, Moment of Inertia Determination and Sensitivity Analysis of an Axial Flux Permanent Magnet AC Motor,” June 2008, U25099.

